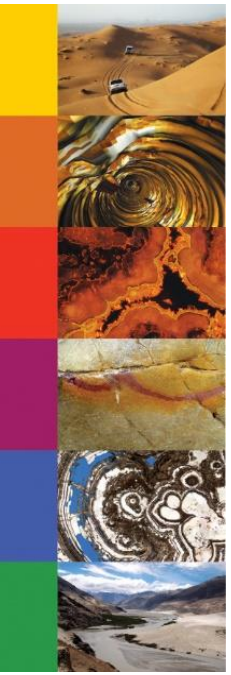

The use of borehole image interpretation in characterising cement nodules and associated nodule-bound micro-fracture distribution in the Mauddud Formation, North Kuwait

Nicolas Foote[1], Daniel Clay[1], Meriem Bertouche[1], Sabry Abd El-Aziz[2], Chao Chen[2], Raja Ramalingam[2], Gahdeer Boland[2] and Mohamed Helmy[3]

1. Badley Ashton and Associates Ltd
2. KOC
3. Shell Kuwait Exploration and Production

Aims of the study

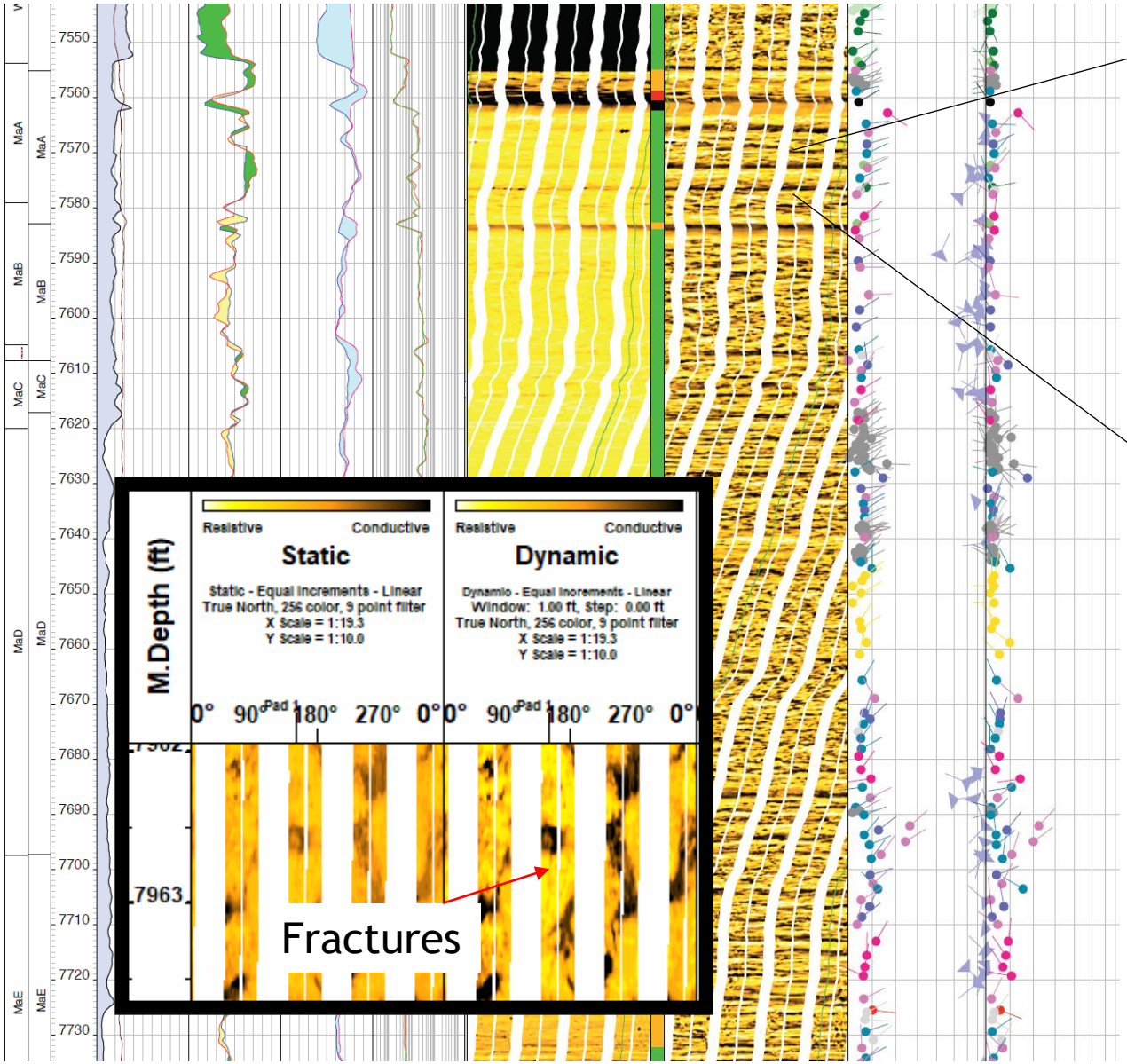

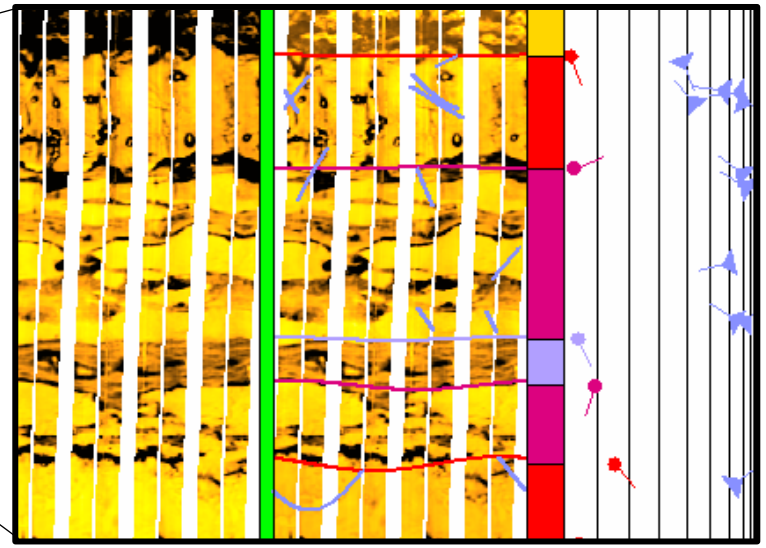

- Minor variation in wireline log response across the carbonate succession
- Interpretation of cement and nodule distribution challenging
- BHI allows detailed description of the reservoir outside of the cored interval

Location map and study dataset

47 imaged wells
22 processed in this study
Dominantly good quality
2 horizontal

A

B

Age		Stage	Formation
Cretaceous	Upper	Maastrichtian	Tayarat Formation
			Qurna Formation
		Campanian	Hartha Formation
		Santonian	Sadi Formation
		Coniacian	Khasib/Mutriba
		Turonian	
		Cenomanian	Mishrif Formation
			Rumaila Formation
			Ahmadi Formation
			Wara Formation
	Lower	Albian	Mauddud Formation
			Burgan Formation
		Aptian	Shuaiba Formation
		Barremian	Zubair Formation

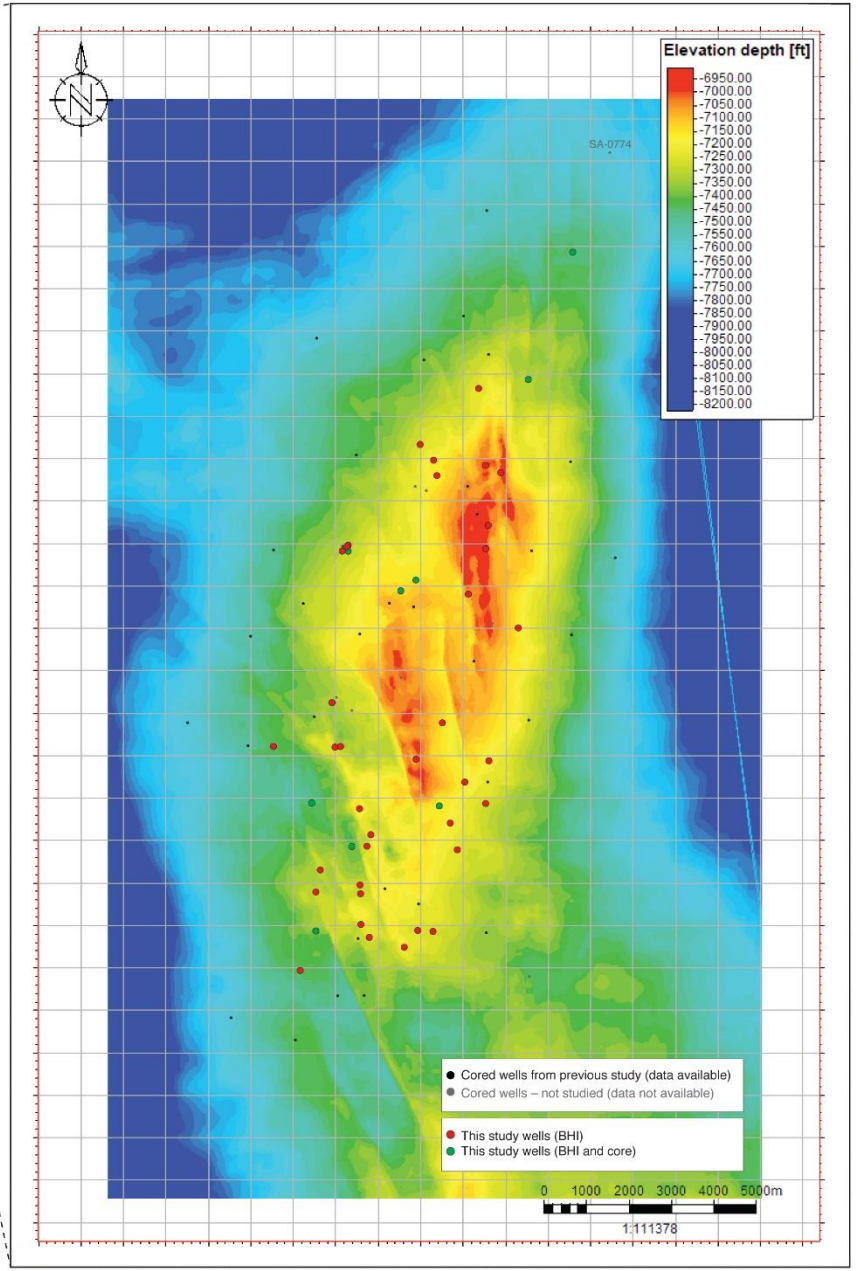

C

Well	Image Type	Processing	Image Quality
1	FMI	Badley Ashton	Moderate
2	FMI	Badley Ashton	Good
3	FMI	Badley Ashton	Good
4	STAR&CBIL	Badley Ashton	Good
5	FMI	Badley Ashton	Good
6	CBIL	Provided	Moderate
7	FMI	Badley Ashton	Good
8	STAR&CBIL	Provided	Good
9	STAR&CBIL	Badley Ashton	Good
10	STAR&CBIL	Badley Ashton	Poor
11	STAR&CBIL	Badley Ashton	Poor
12	STAR&CBIL	Provided	Good
13	STAR&CBIL	Badley Ashton	Moderate
14	CBIL	Provided	Moderate
15	STAR&CBIL	Provided	Good
16	FMI	Badley Ashton	Good
17	FMI	Badley Ashton	Good
18	STAR&CBIL	Badley Ashton	Good
19	FMI	Badley Ashton	Good
20	FMI	Badley Ashton	Good
21	STAR&CBIL	Provided	Moderate
22	EMI	Provided	Moderate
23	FMI	Badley Ashton	Good
24	EMI	Provided	Good
25	FMI	Badley Ashton	Good
26	FMI	Provided	Good
27	FMI	Badley Ashton	Good
28	FMI	Badley Ashton	Good
29	STAR&CBIL	Provided	Good
30	STAR&CBIL	Provided	Good
31	FMI	Provided	Good
32	STAR	Badley Ashton	Good
33	FMI	Provided	Good
34	STAR&CBIL	Provided	Good
35	FMI	Badley Ashton	Good
36	FMI	Badley Ashton	Good
37	STAR&CBIL	Provided	Moderate
38	STAR&CBIL	Provided	Moderate
39	STAR&CBIL	Provided	Moderate
40	STAR&CBIL	Provided	Moderate
41	EI&CBIL	Provided	Moderate
42	EMI	Provided	Good
43	FMI-HD	Provided	Good
44	STAR&CBIL	Provided	Moderate
45	FMI	Provided	Good
46	FMI	Provided	Good
47	FMI-HD	Provided	Good

Image facies scheme

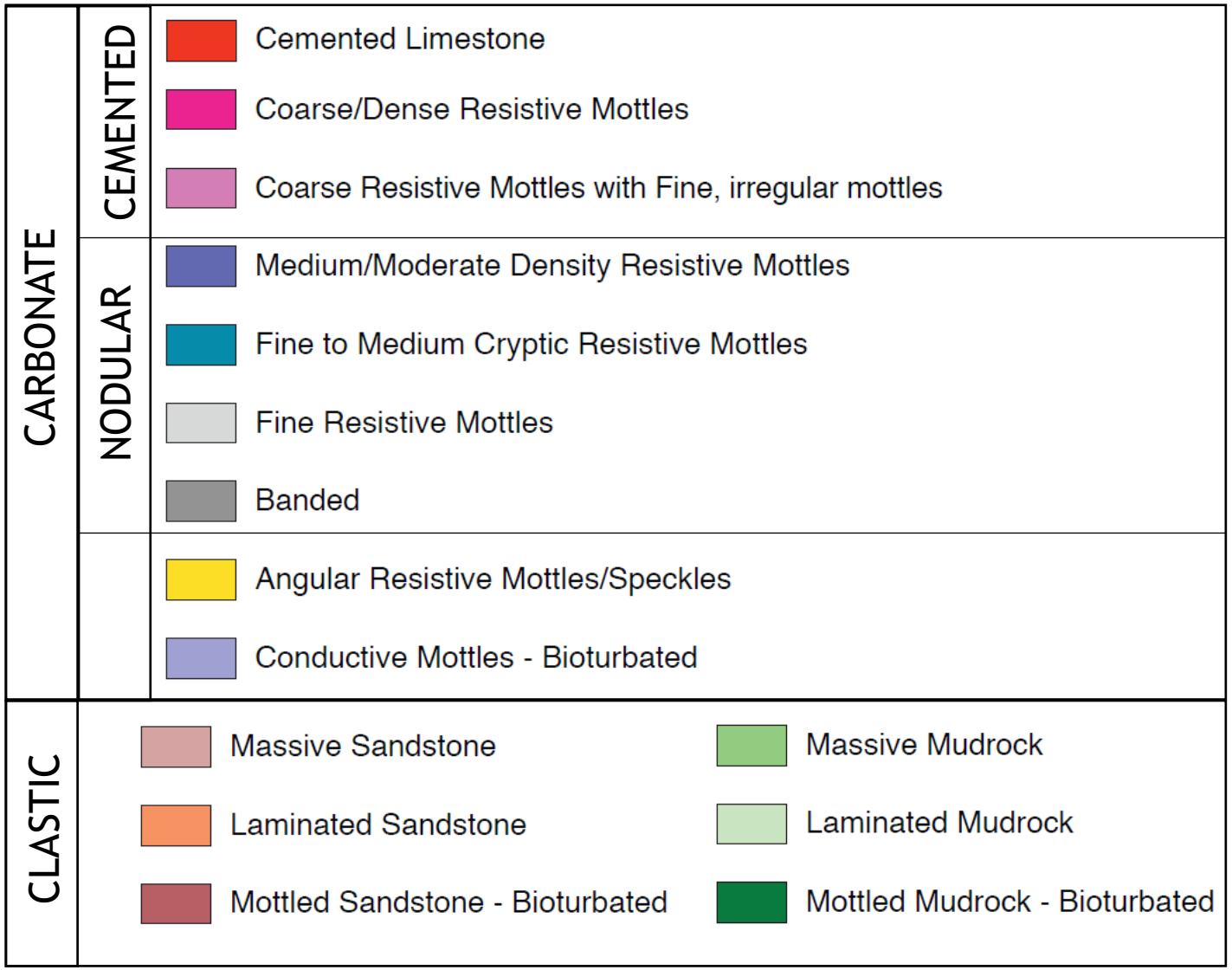

- The image facies scheme groups limestone image characteristics into cemented and nodular categories facilitating large scale analysis whilst also maintaining a highly descriptive scheme
- Examples of image facies showing the key sedimentological and structural observations from BHI that can be extrapolated into uncored intervals are presented in the next few slides

Cemented limestone

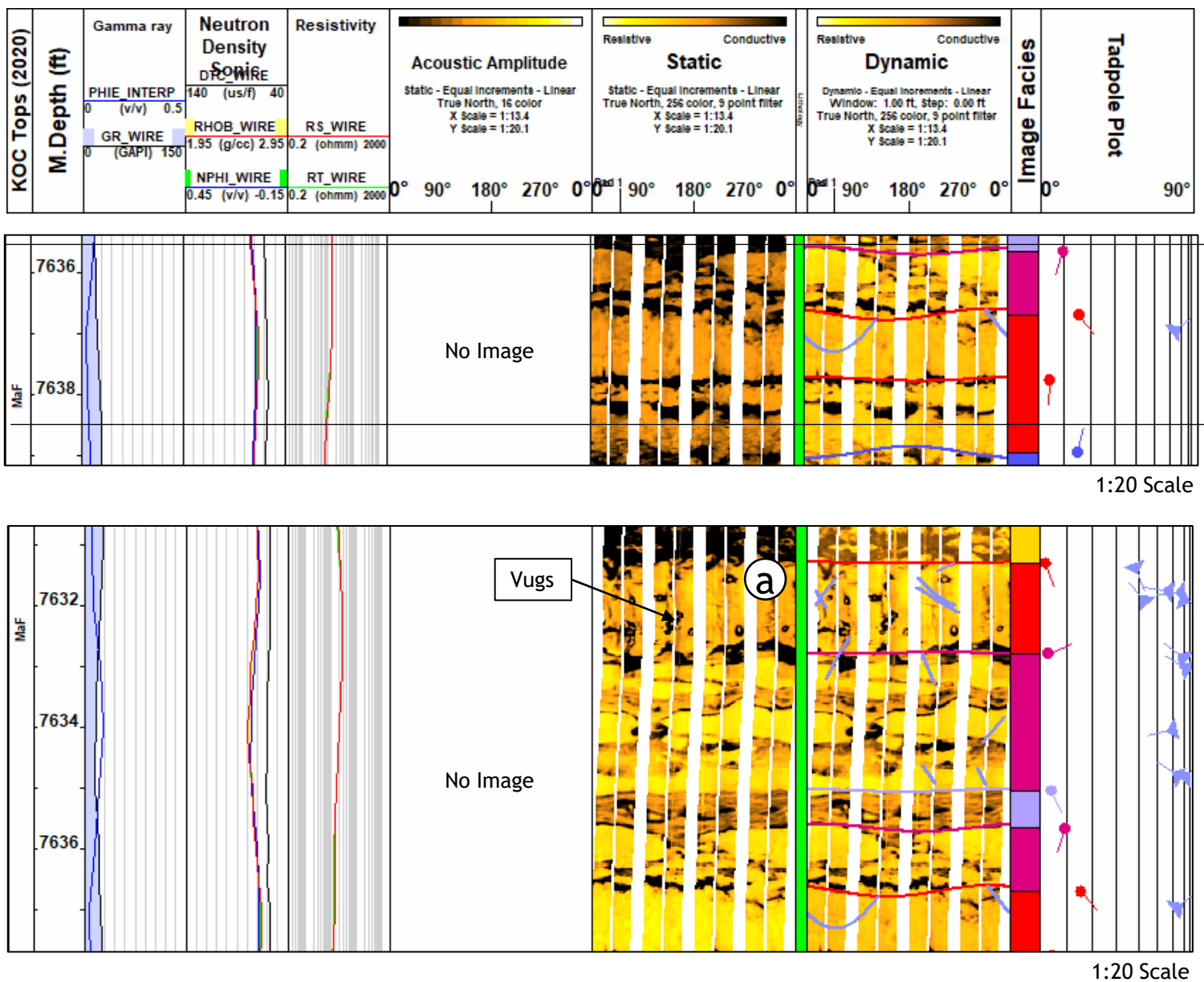

Cemented limestone (rLc)

BHI Character: Expressed as a highly resistive, borehole-spanning image facies that is typically in the foot to deci-foot scale. Microfractures are readily seen in this image facies as well as conductive mottles which are interpreted to be vugs (a).

Conventional Log Character: Log response is often variable, however, a relative low GR and closed 'limestone' N/D response is typical. Slight increases in wireline resistivity logs are observed.

Core Character: This image facies in core corresponds to a fully cemented limestone, with some potential bioturbation imprint still visible. Microfractures in cemented sections of core are common and are seen at much higher densities than in image due to the different resolutions of the two datasets.

Coarse/high density resistive mottles

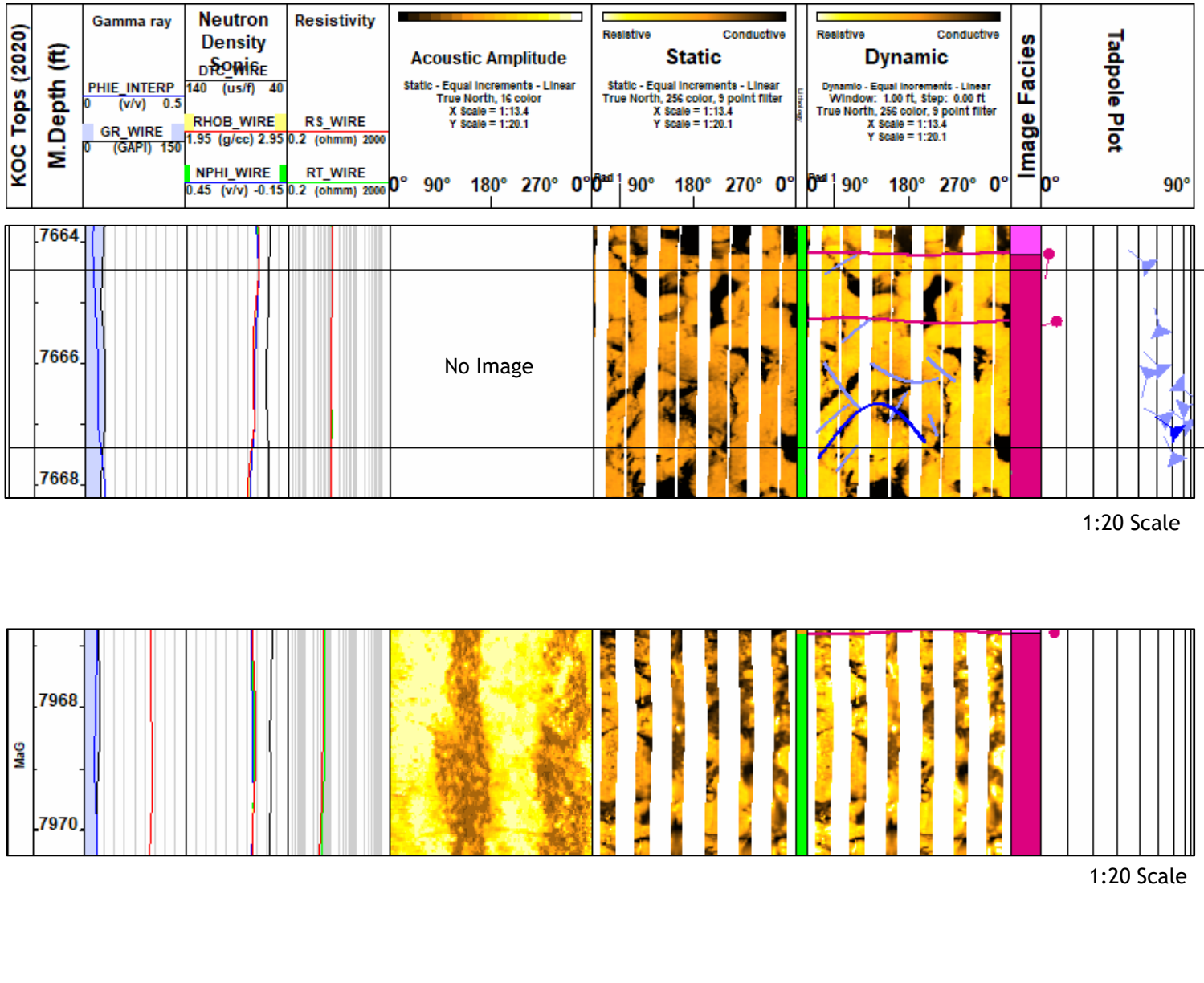

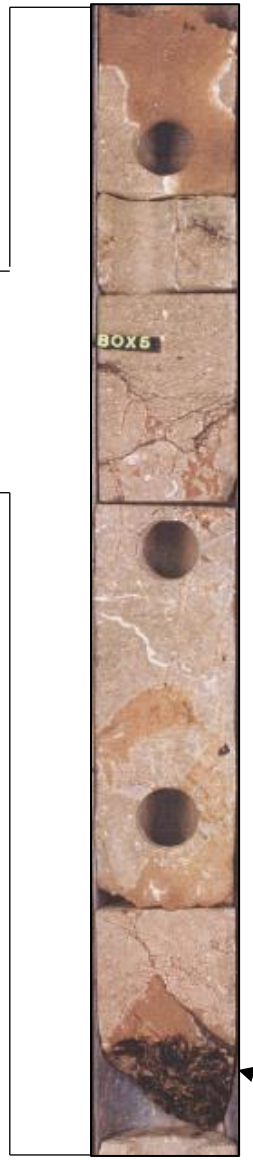

Oil stained fracture, non-continuous conductive fracture in BHI

Coarse/high density resistive mottles (rLcm)

BHI Character: Constantly large resistive mottles, often tightly packed with conductive gaps between. Microfractures are readily seen in this image facies.

Conventional Log Character: As with the cemented limestone image facies, log response is variable, however, a relative low GR and closed 'limestone' N/D response is typical. Slight increases in wireline resistivity logs are observed.

Core Character: This image facies in core is expressed by abundant, course cemented patches with some preserved porosity. In some instances, conductive seams in the image facies correspond to clay seams.

Medium/moderate density resistive mottles

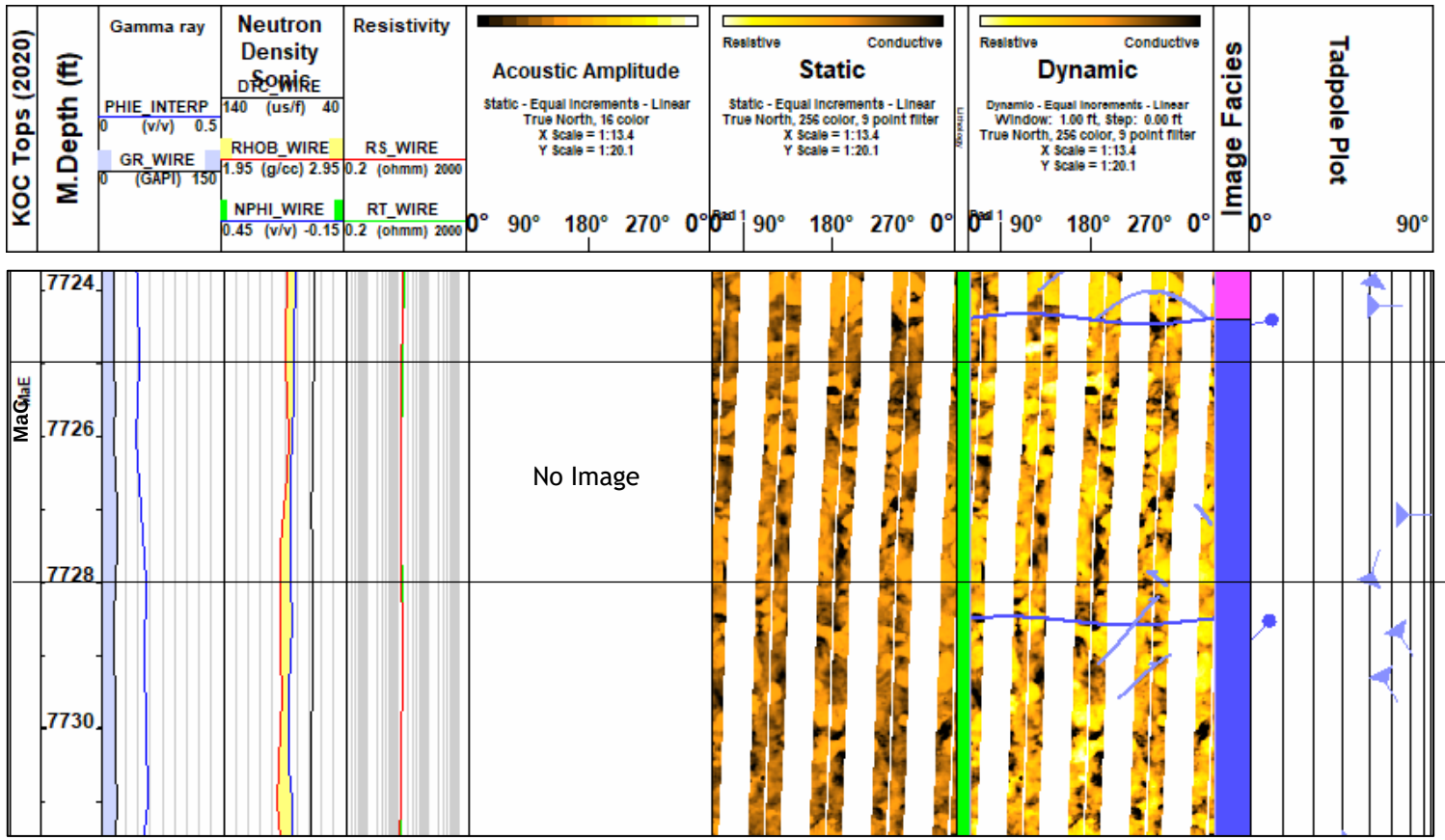

Core to log shift = 5ft 7720ft dd

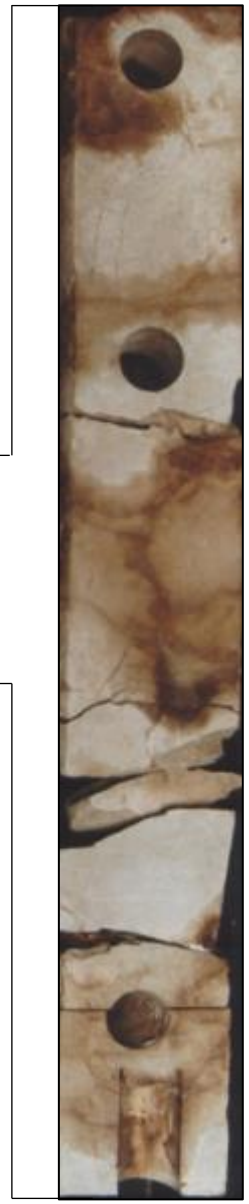

7723ft dd

Medium/moderate density resistive mottles (rLmm)

BHI Character: Medium size resistive mottles often with conductive space observed between them as a result of moderate nodule density. Microfractures are observed and mostly bound in resistive mottles.

Conventional Log Character: As with the cemented limestone image facies, log response is variable, however, a relative low GR and closed 'limestone' N/D response is typical.

Core Character: In core, resistive mottles are associate to heavily cemented limestone. Inter-nodular areas are commonly more porous and oil stained. Microfracturing is observed in these cemented nodules which are also oil stained.

Angular mottling - Rudists/skeletal fragments

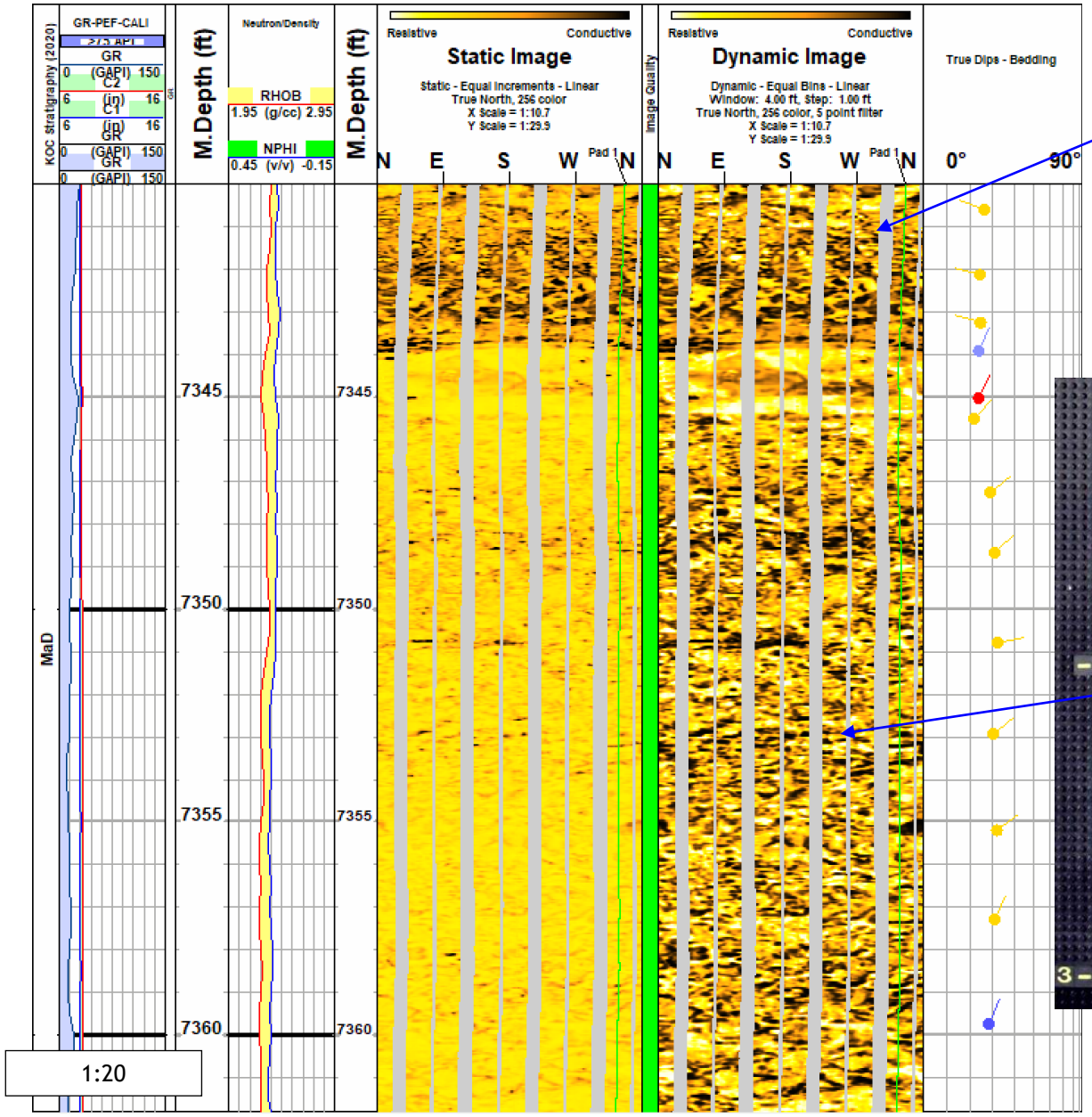

Abundant cm-scale (up to 8cm) rudist fragments in clean packstone/floatstone.

7345-7359ft: common (small) fragmented rudists:

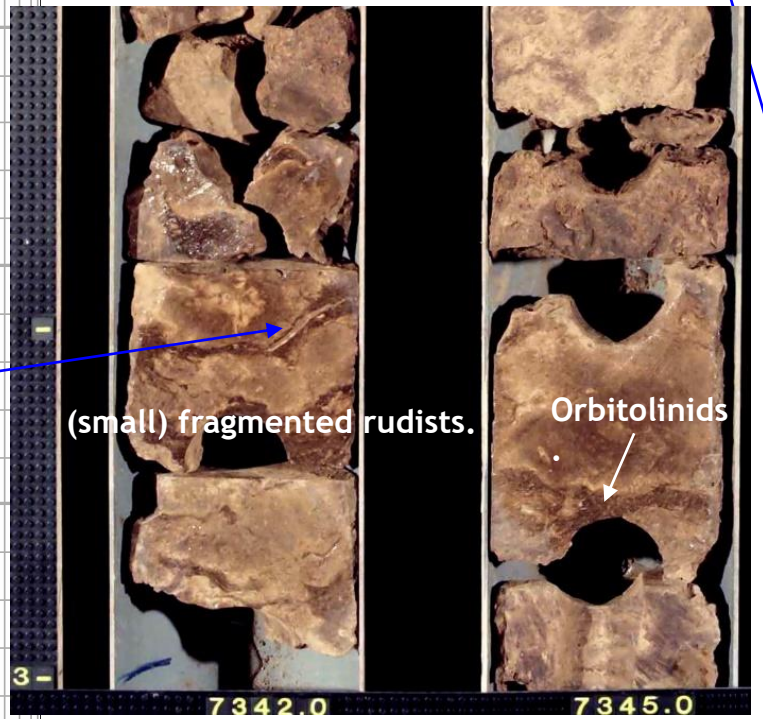

Rudists decrease in abundance downwards.

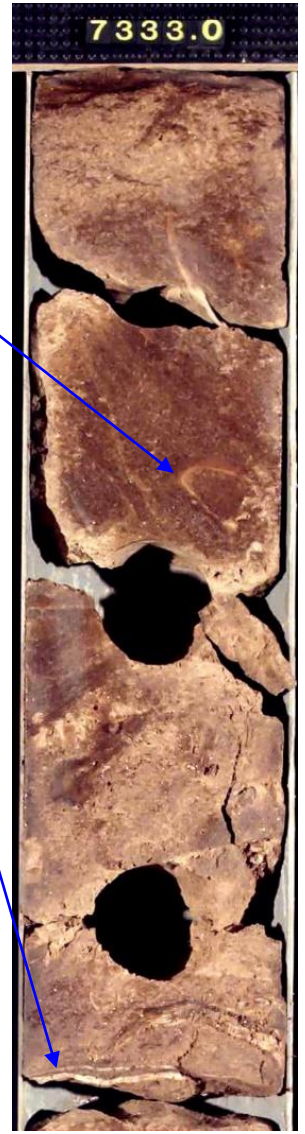

Cemented layers - MaF example

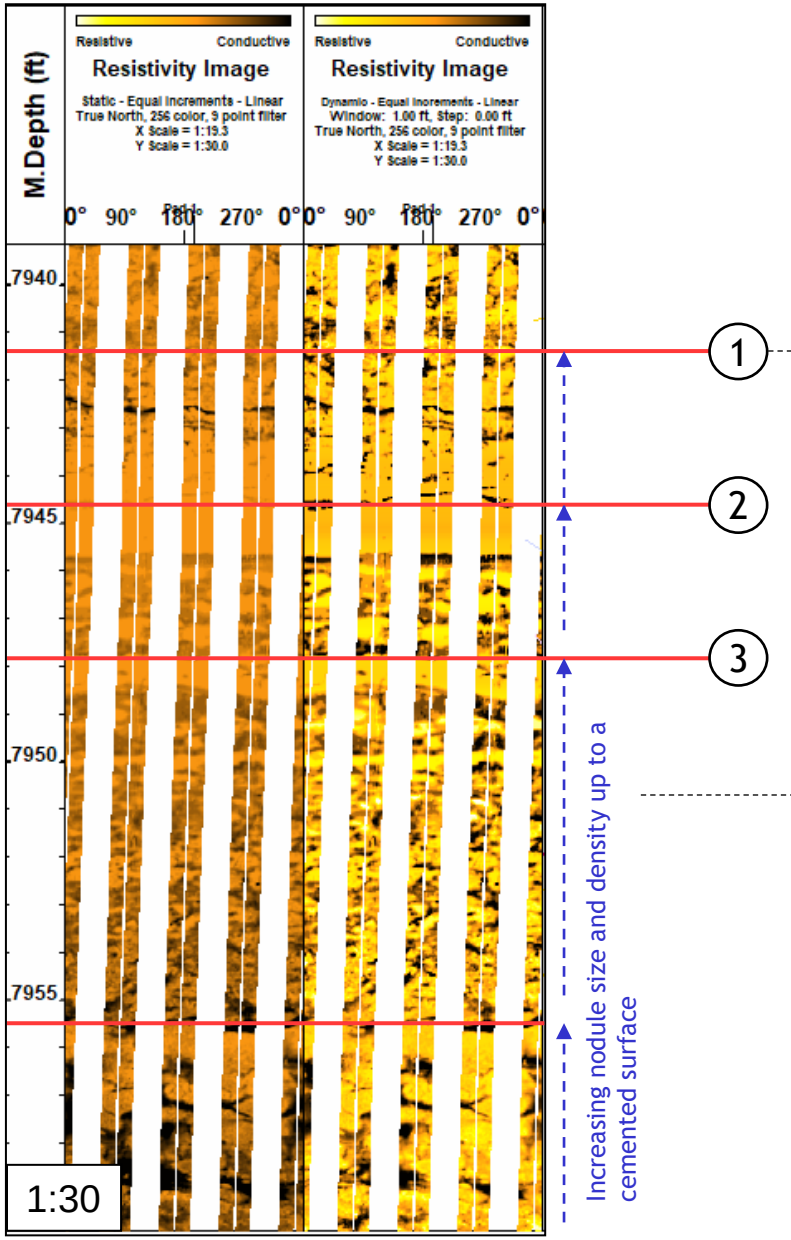

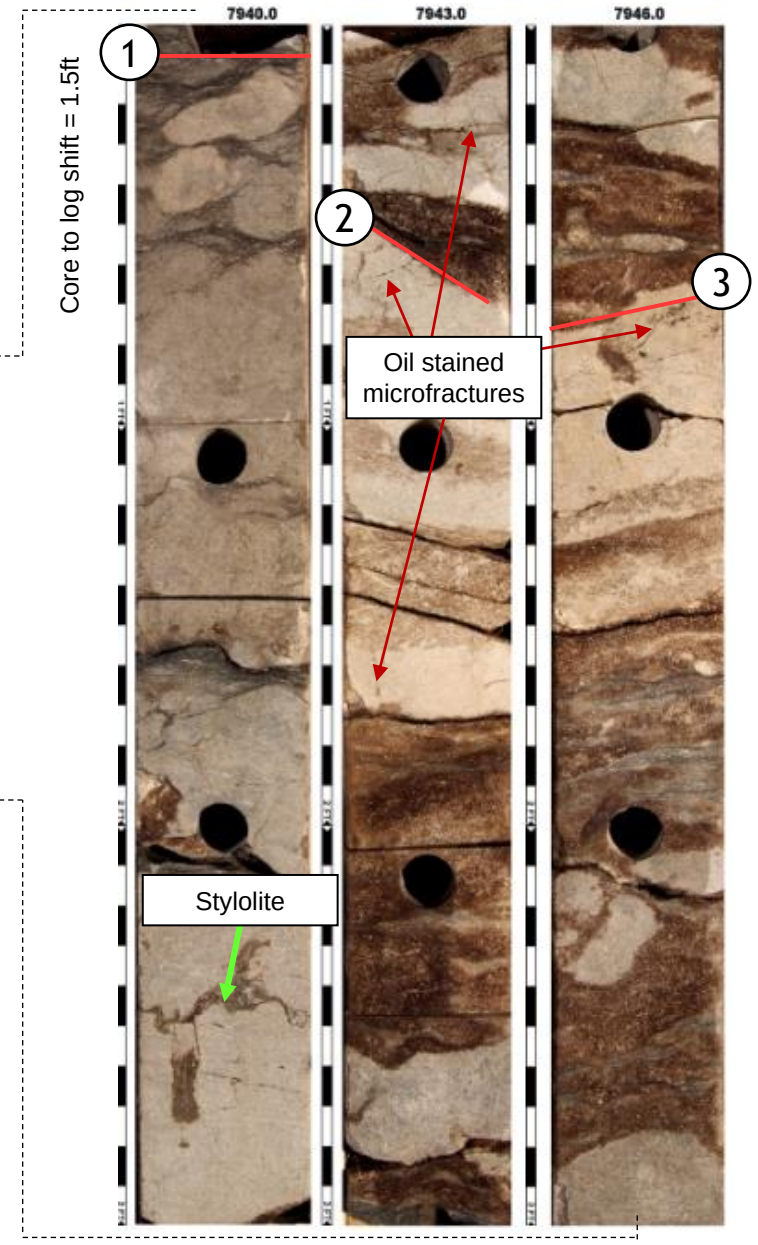

- Cementation clearly has an impact on hydrocarbon flow within the Mauddud. Microfractures are observed, in this core example within the MaF below image resolution, however, none appear to cross-cut the full cemented section
- Core calibration shows differential oil staining associated with this cementation trend
- Identification of these image facies in BHI has been used to characterise reservoir heterogeneity as seen in Figure 5 and summarised on the next slide with the distribution of micro-fractures in this context also explored

Image facies distribution

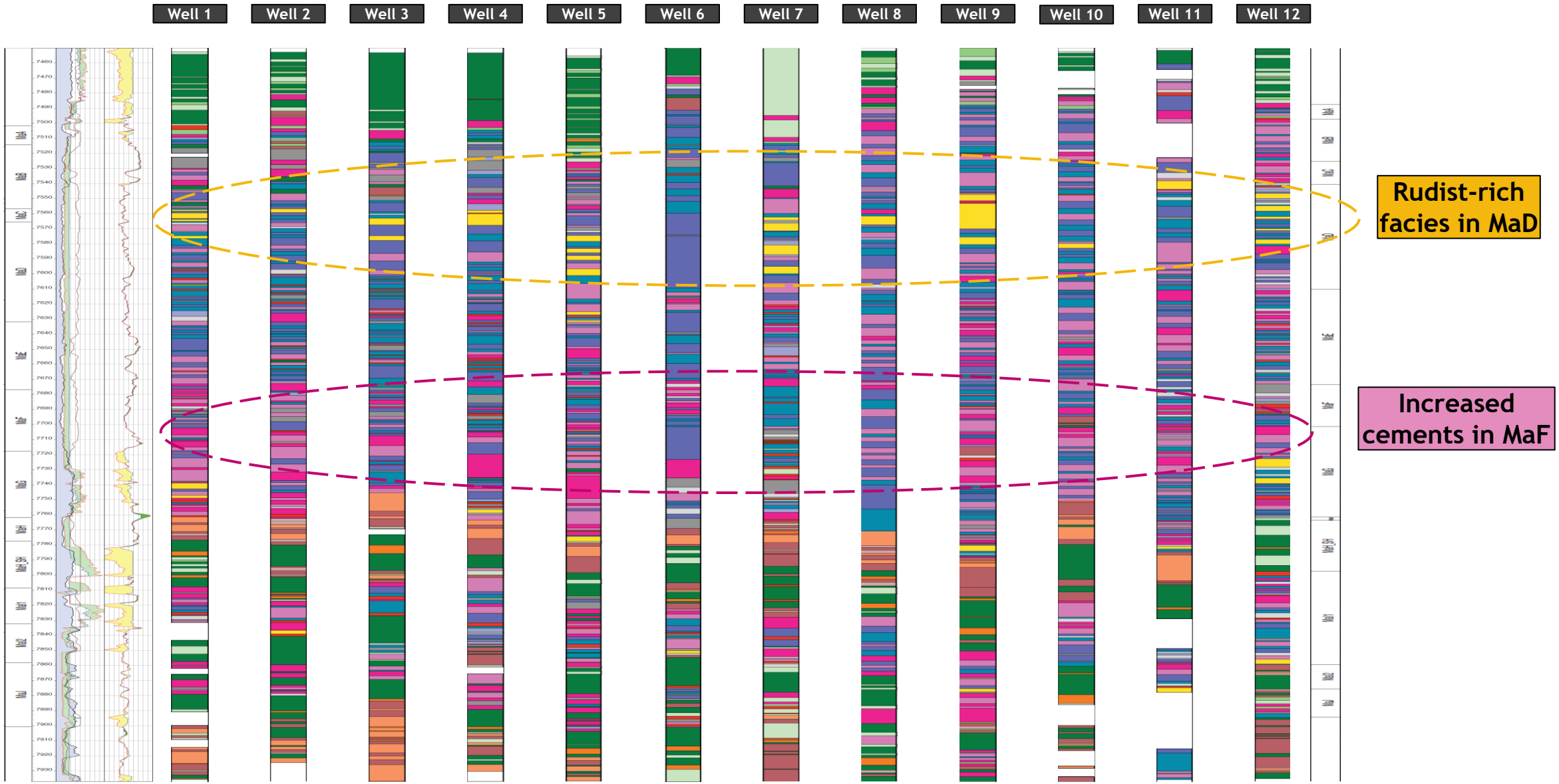

Cement distribution maps

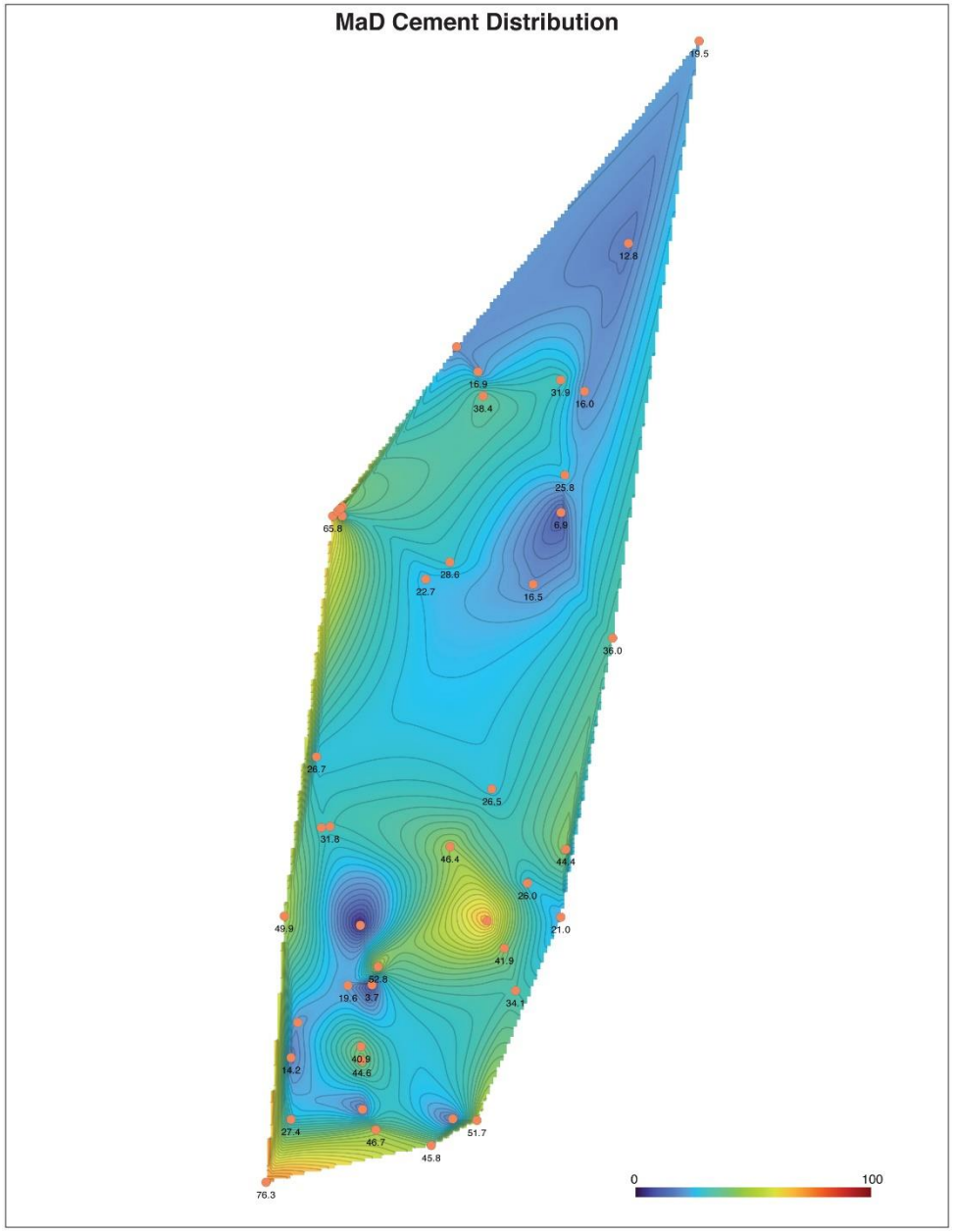

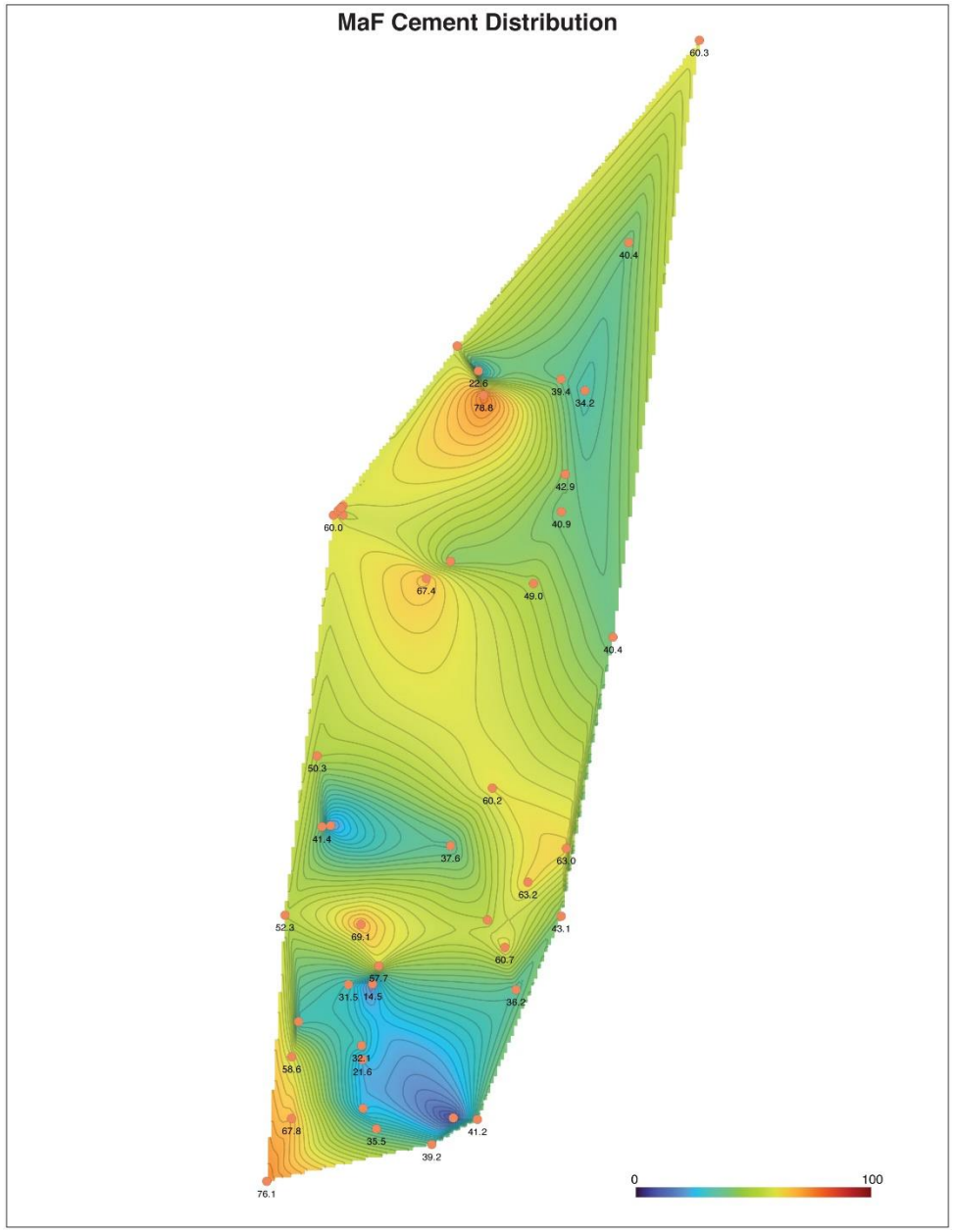

Cement maps per reservoir layer

MaA

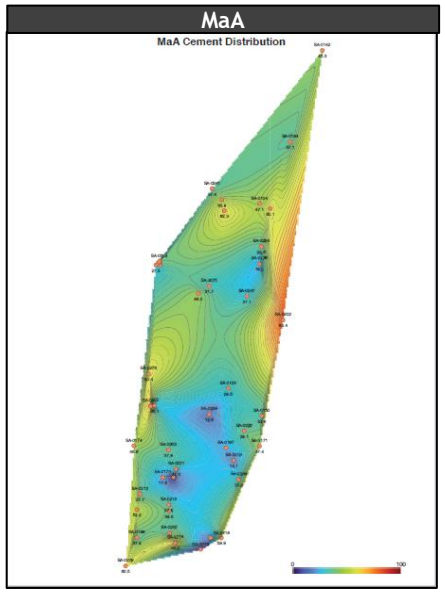

MaB

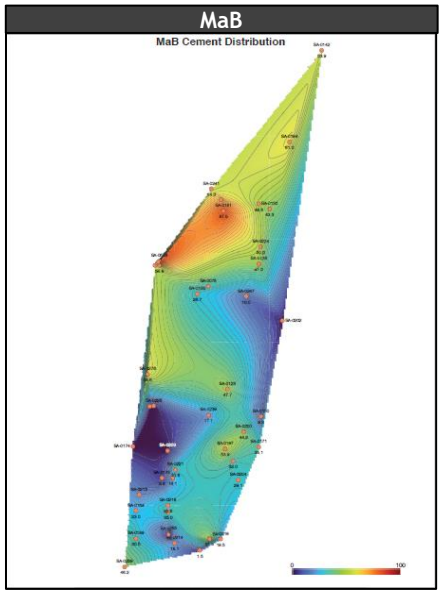

MaC

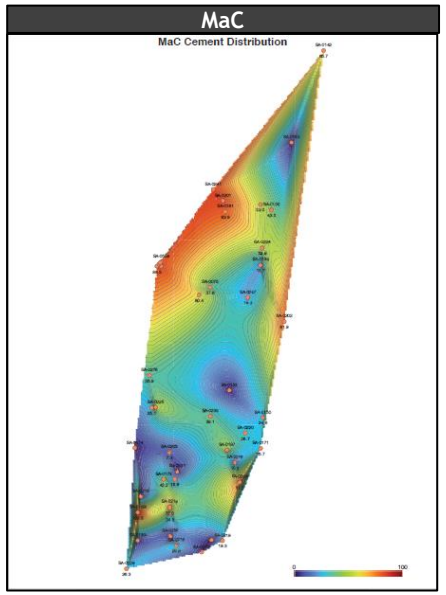

MaD

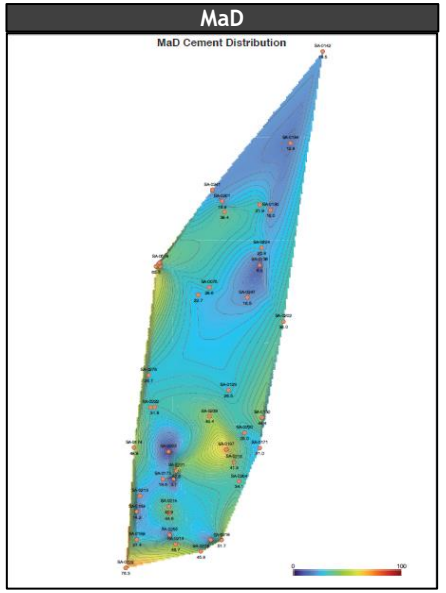

MaE

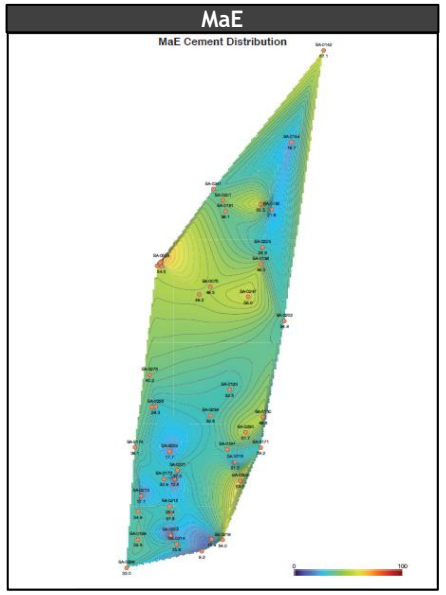

MaF

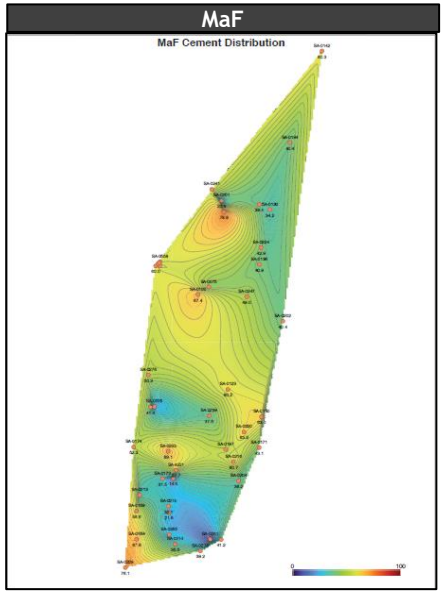

MaG

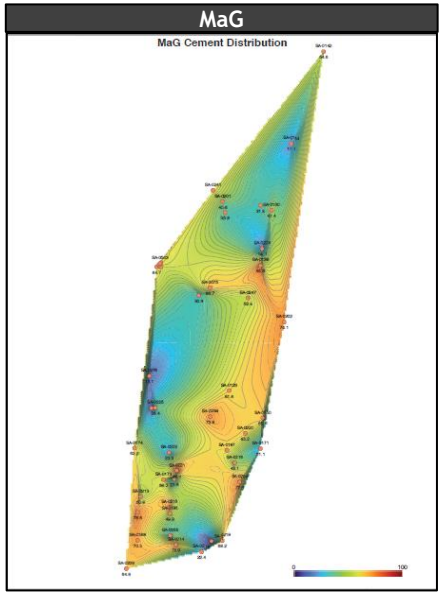

MaH

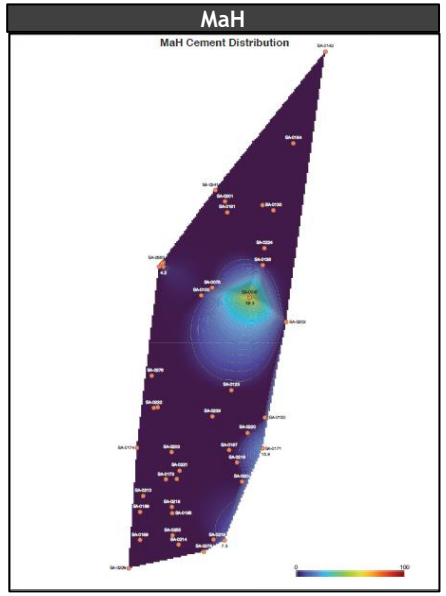

MaH-SH

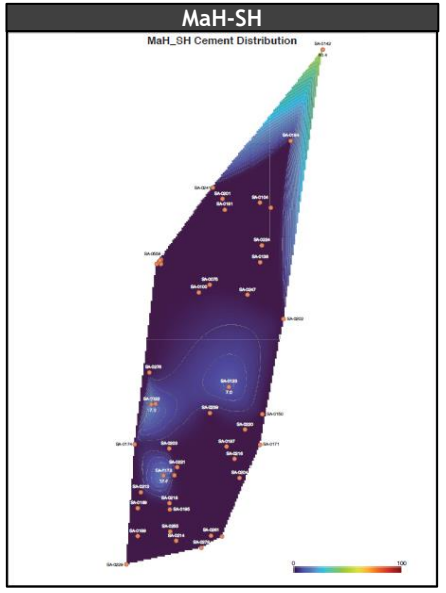

MaI1

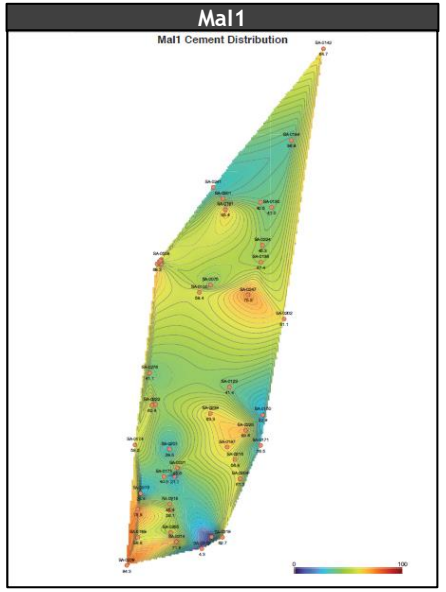

Microfractures - core calibration

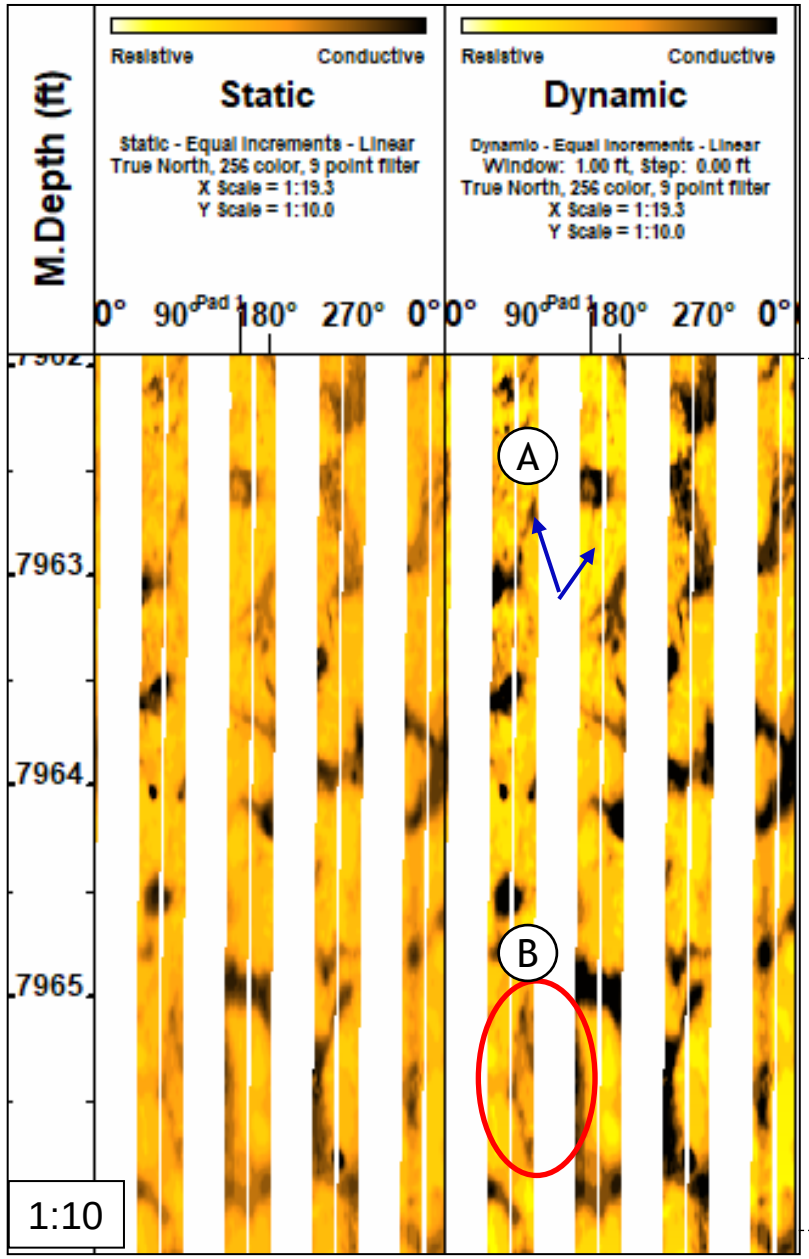

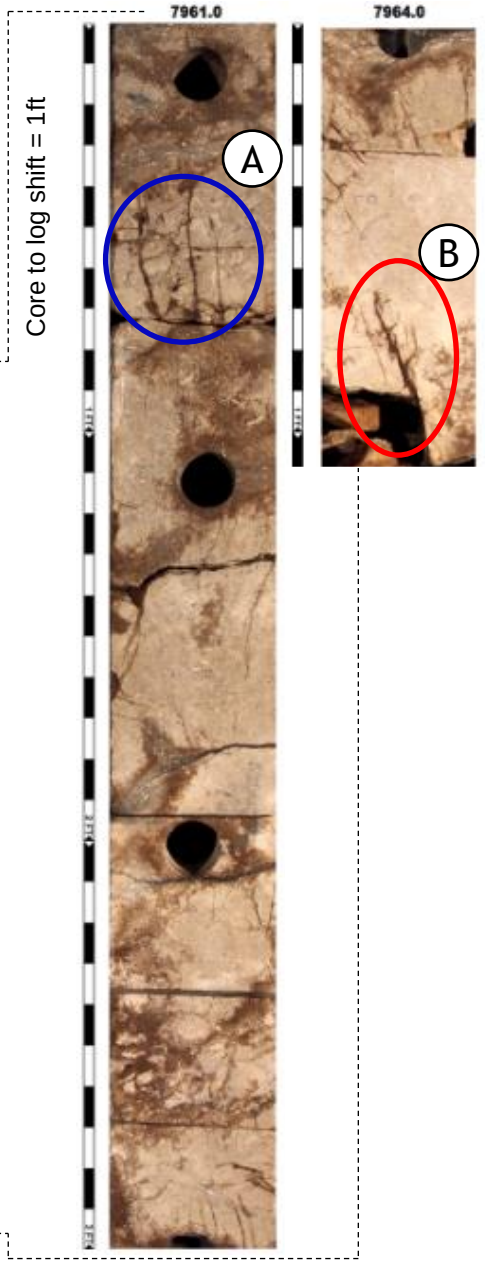

- Core observations show oil stained fractures cross-cutting cemented nodules
- In this core example, these are well connected and provide conduits for flow
- These microfractures are picked out in BHI enabling orientation of the network
- The high density of mircrofractures seen in core is not reflected in BHI
- Observations of BHI show clusters of microfractures preferentially occurring in cemented and coarse/dense image facies as well as some nodular cemented image facies

Core *vs* BHI microfractures fracture density

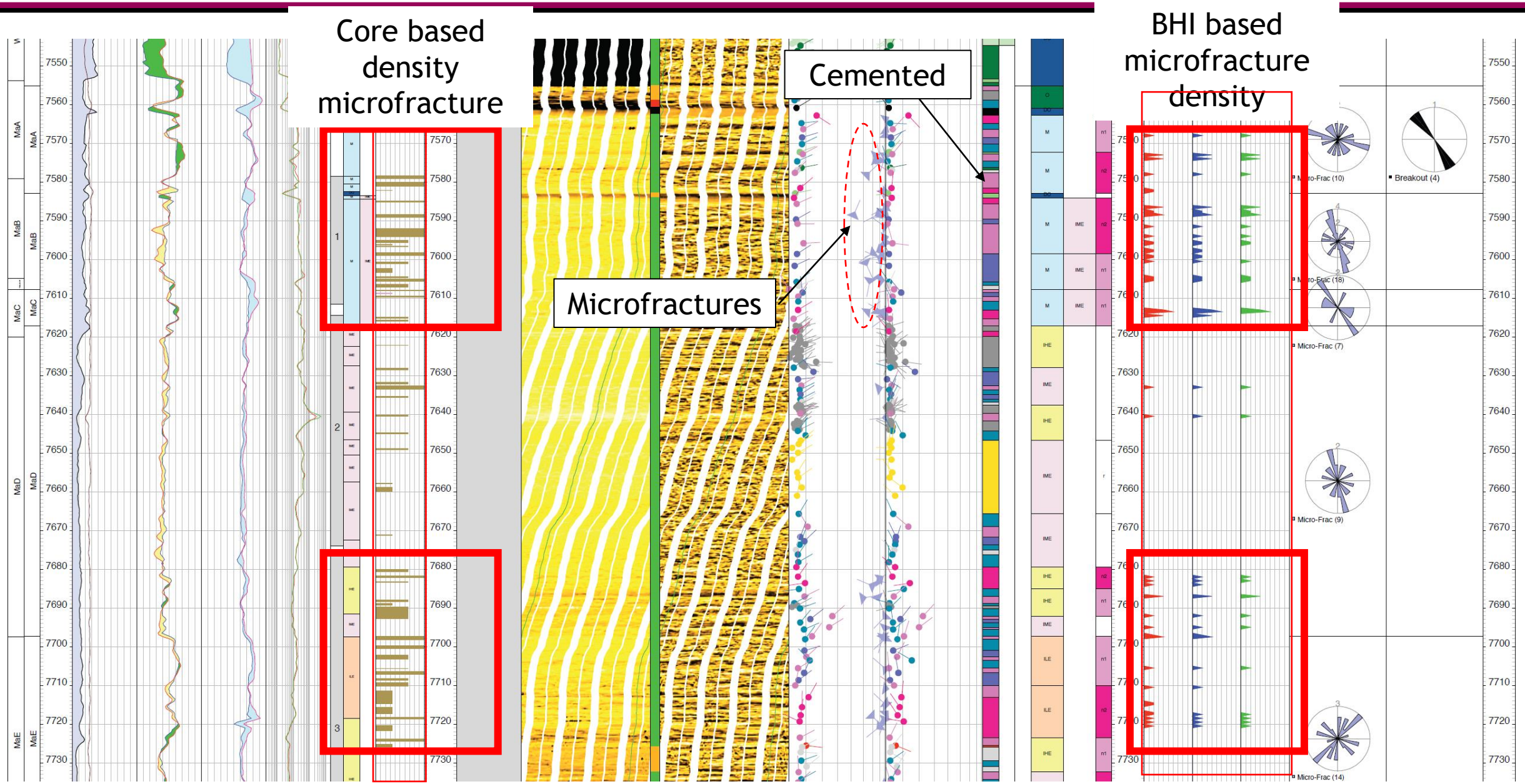

Cemented zones and microfracture distribution

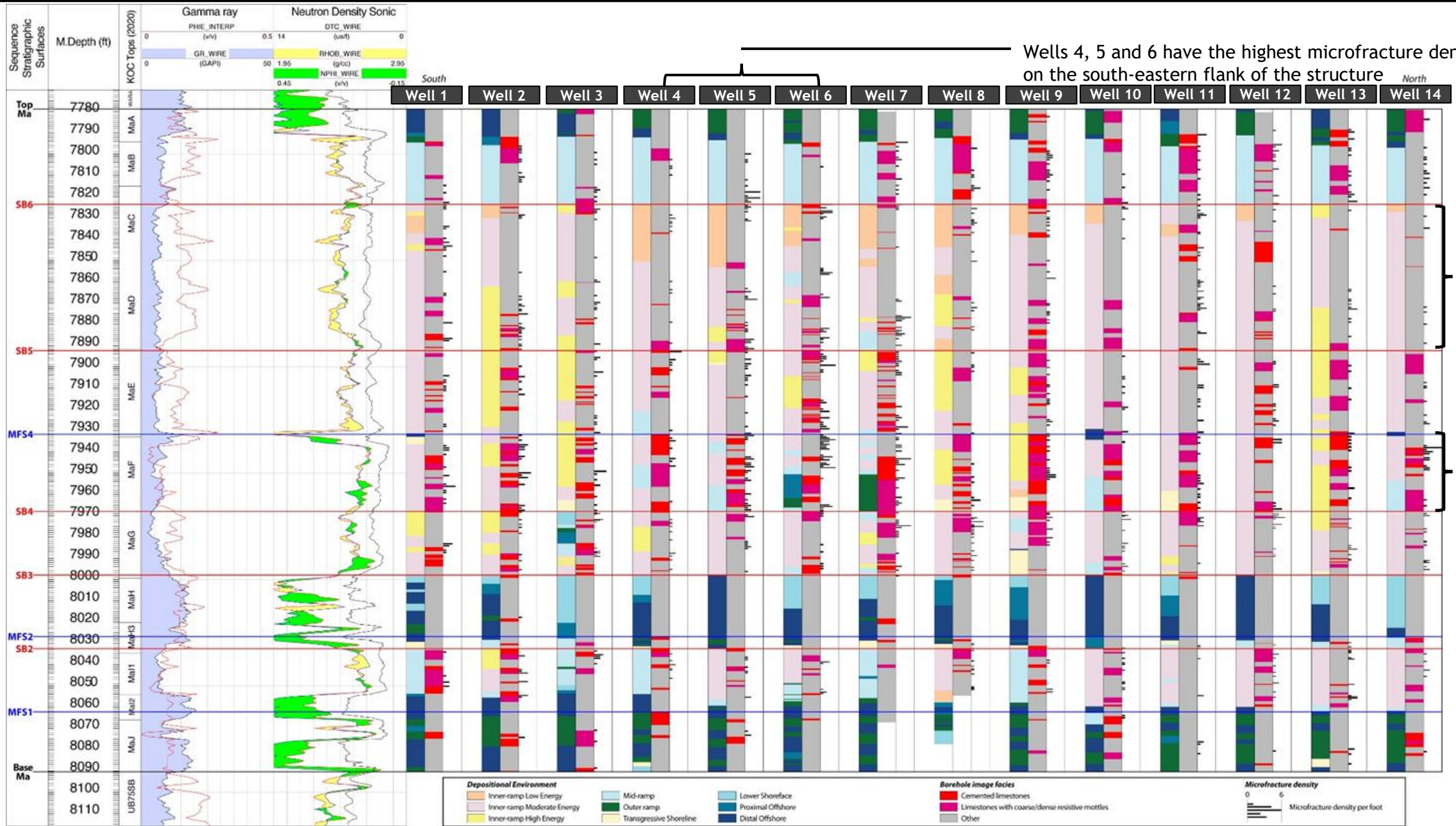

Wells 4, 5 and 6 have the highest microfracture densities, located on the south-eastern flank of the structure

Microfracture density in the MaC and MaD is low aside from in more cemented sections

The MaF has a greater concentration of the two most cemented image facies as well as an increase in microfracture density

Conclusions

- The cement distribution may have a link to sedimentology which is still being studied
- Clear relationship between amount of cement and frequency of microfractures
- In the upper intervals of the Mauddud fracture frequency is greatest on the flanks of the field where cement is more intense
- Microfractures are more common at the crest of the structure in the lower intervals (MaF and MaG) where cement is more pervasive
- Primary porosity in the crest of the structure is preserved, although nodule bound microfractures have the potential to increase secondary porosity where cementation is more pervasive